

# Theoretical and Experimental Studies on Blast Wave Propagation in Air

Vedula Dharma Rao,<sup>[a]</sup> Adapaka Srinivas Kumar,<sup>\*,[b]</sup> Kadiyam Venkateswara Rao,<sup>[b]</sup> and Veerapaneni S. R. Krishna Prasad<sup>[c]</sup>

**Abstract:** High pressure and temperature are produced when high explosives are detonated in open air. The heat of detonation of the explosive compound, peak pressure, and temperature of the blast wave are important blast parameters. A blast wave generated due to explosion propagates into the air medium at supersonic speed until the pressure in the blast zone is released completely. The intensity of the impact by the blast wave on any intervening solid object depends on the blast parameters and the speed of propagation of the blast wave. A theoretical analysis is carried out to predict the pressure produced in the expanding blast zone as function of distance and time by

analytically solving the governing equations. The initial peak pressure and temperature of blast wave, which are required in the theoretical analysis, were calculated making use of the blast wave theory. For comparison, experiments were conducted by detonating different weights of high explosives, and pressures were recorded at various distances from the blast point. The high explosives used in the experiments were TNT (0.045, 0.5, 1, 15, and 40 kg) and Composition B (0.045, 0.5, 1, and 15 kg). The theoretical results are validated by comparison with the experimental data and empirical equations available in literature.

**Keywords:** Blast in air · High explosives · Shock wave · Gas expansion · Pressure · Blast wave theory

## 1 Introduction

Detonation of high explosives generates shock waves associated with exothermic chemical reaction. The detonation is considered complete, when the detonation wave has broken through the surface of the charge. When the detonation wave reaches the surface of the charge, the air immediately outside the charge is rapidly accelerated; generating what is called a “blast wave” [1]. The blast wave, which is at very high pressure and temperature then expands into the stagnant air until the pressure is fully relieved and reaches ambient. The study of propagation of blast waves in air assumes importance in military environment. The peak pressure and temperature produced in the blast zone can be estimated by calculating the stagnation pressure and temperature ahead of the blast wave [2,3]. The pressure behind the blast wave depends on the heat of detonation of the explosive [3,4]. It is generally difficult to measure the blast pressures at the close vicinities of points of detonation of explosives [5]. So is the case of measurement of temperature [6]. The theoretical analysis carried out for the problem of movement of blast wave in air enabled estimation of the pressures produced in the expanding blast zone as functions of distance and time at close proximity of point of detonation.

## 2 Theoretical Analysis

A blast of an explosive occurs in a stationary medium of atmospheric air. The detonation wave, produced at the blast point, moves forward into the infinite medium of stagnant air. The blast gas expands in all directions uniformly. Hence, the blast gas zone is assumed to be spherical in shape. Its shape also depends on the shape and weight of the explosive charge [7], mode of initiation, properties of the ambient medium, etc. Hence, a plane wave front is also considered in the analysis to represent a limiting case. The physical model showing the spherical and plane wave fronts is presented in Figure 1.

The problem is formulated as follows: When a high explosive is detonated, a blast zone gets created, which ex-

[a] V. Dharma Rao  
Department of Mechanical Engineering  
GVP College of Engineering  
Visakhapatnam – 530048, India

[b] A. Srinivas Kumar, K. Venkateswara Rao  
Naval Science and Technological Laboratory  
Vigyan Nagar  
Visakhapatnam-530027, India  
\*e-mail: adapakaeskay@yahoo.com

[c] V. S. R. Krishna Prasad  
Anil Neerukonda Institute of Technology and Science  
Visakhapatnam – 530054, India

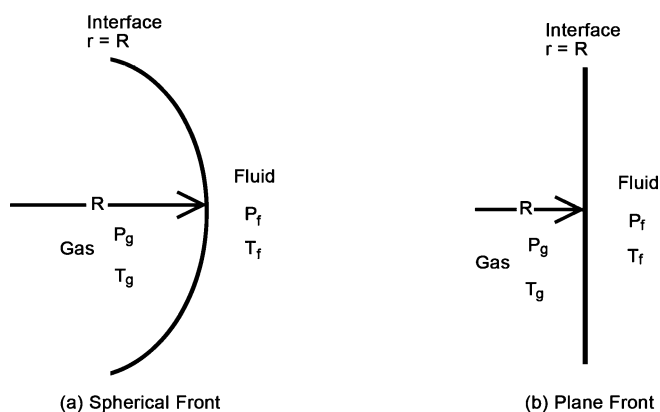


Figure 1. Physical model for the movement of the blast wave.

pands into the stagnant medium, which is air in the present study. The radius of the blast zone, as it is created is named as “initial radius” and is represented as  $R_0$ , which is independent of charge dimensions. The pressure in the blast zone is maximum at this stage (where  $R$  is minimum). As the blast wave expands (increase of  $R$ ), the pressure in the blast zone reduces until it equals the ambient pressure. The initial pressure and temperature of the gas in the blast zone are  $p_{g0}$  and  $T_{g0}$ , respectively. The ambient air is at a constant pressure equal to  $p_f$  and, if treated as an infinite heat sink, its temperature and density remain constant at  $T_f$  and  $\rho_f$ , respectively.

Heat is dissipated from the blast zone by convection and radiation to the surrounding fluid. The pressure and temperature of the gas in the blast zone decrease as the wave front moves forward. The variables which change with time are the radius of the blast gas sphere ( $R$ ), pressure ( $p_g$ ), temperature ( $T_g$ ), and density ( $\rho_g$ ) of the gas in the blast zone. It is assumed that the gas in the blast zone behaves like a perfect gas and obeys the ideal gas law. The authors presented in their previous work in detail the theoretical analyses involving derivation of governing differential equations for (i) Motion of air adjacent to the detonation wave front; (ii) heat balance at the gas-to-fluid interface; and (iii) pressure and temperature in blast zone. Evaluations of initial conditions for pressure and temperature have also been presented in reference [8]. Hence, only the governing equations are presented in this paper for detonation of explosives in air medium.

### 2.1 Motion of Air Adjacent to the Blast Wave Front

The atmospheric air which is adjacent to the blast wave front (at  $r=R$ ) moves with the same velocity as the wave front moves. Thus, the velocity of the fluid at  $r=R$  is equal to  $u_i$  where  $u_i = dR/dt$ . However, the bulk fluid, which is away from the gas, is at rest. The motion of air is governed by (i) the continuity and (ii) the momentum balance equations (neglecting the viscous force) in spherical coordinates as shown below [8]:

$$\frac{\partial}{\partial r} (r^2 u) = 0 \quad (1)$$

$$\rho_f \left( \frac{\partial u}{\partial t} + u \frac{\partial u}{\partial r} \right) = - \frac{\partial p_f}{\partial r} \quad (2)$$

The boundary conditions (for  $t > 0$ ) are listed as follows:

$$u = u_i \text{ at } r = R, \text{ and } u \rightarrow 0 \text{ as } r \rightarrow \infty \quad (3)$$

The final equation in simplified integral form can be given as [8]:

$$\frac{d}{dt} \int_R^\infty u \, dr + u_i \frac{dR}{dt} - \frac{u_i^2}{2} = \frac{p_{f,i} - p_f}{\rho_f} \quad (4)$$

$p_{f,i}$  is the pressure of the fluid at the gas-to-fluid interface. The force balance at the gas-to-fluid interface is given by

$$\frac{d^2 R}{dt^2} + \frac{3}{2R} \left( \frac{dR}{dt} \right)^2 = \frac{p_g - p_f}{\rho_f R} - \frac{2\sigma_s}{\rho_f R^2} \quad (5)$$

### 2.2 Heat Balance at the Gas-to-Fluid Interface ( $r=R$ )

Heat is transferred from the gas to the fluid by convection and radiation during the expansion of gas. A lumped heat capacity model is used for the blast zone in deriving the heat balance equation. Two extreme cases of spherical wave expansion and plane wave propagation in air are proposed. The heat generated in the blast zone (volume) is dissipated through the surface of the wave (area). The initial shapes of blast waves depend on the geometry and mode of initiation of explosive to a great extent. In the present case, for spherical wave, after the equation is rearranged a quotient “3” appears in the denominator. In the case of plane wave, the quotient is equal to “1”. When these two cases are represented in a single equation, the extremes of sphere and plane waves are represented as “3” and “1”, respectively, naming them as shape factors, “ $C$ ”. The equation of heat balance at the gas-to-air interface, i.e., at  $r=R$ , is as follows, considering both plane as well as curved wave fronts [8]:

$$\rho_g T_g \frac{dR}{dt} + \frac{R}{C} \frac{d}{dt} (\rho_g T_g) = - \frac{1}{c_{pg}} [h(T_g - T_f) + \epsilon \sigma_r (T_g^4 - T_f^4)] \quad (6)$$

where the curvature is  $C=3$  for spherical wave front and  $C=1$  for plane wave front. A value between 1 and 3 represents a curved front. As defined earlier,  $R$  is the distance of the gas-to-air interface measured from the blast point. The gas heat capacity is shown as  $c_{pg}$  and convection heat transfer coefficient as  $h$ .

## 2.3 Pressure in the Blast Zone

Since the gas is assumed to obey ideal gas law, the following relation can be obtained between the gas density  $\rho_g$  and temperature  $T_g$ .

$$\frac{\rho_g}{\rho_f} = \frac{p_g}{p_f} \frac{T_f}{T_g} \quad (7)$$

$\rho_f$ ,  $p_f$ , and  $T_f$  are the density, pressure and temperature of the ambient fluid, which is air.

As the gas expands the pressure decreases and finally becomes equal to the pressure of the ambient air. Polytropic expansion of gas is assumed in the blast zone.  $p_g$ , the gas pressure and  $\rho_g$ , the gas density are as given by the following equation in terms of  $T_g$ .

$$\frac{p_g}{p_f} = \left( \frac{T_g}{T_f} \right)^{\frac{n}{n-1}} \quad (8)$$

$$\frac{\rho_g}{\rho_f} = \left( \frac{T_g}{T_f} \right)^{\frac{1}{n-1}} \quad (9)$$

When Equation (8) and Equation (9) are used to substitute for  $p_g$  and  $\rho_g$  in Equation (5) and Equation (6), respectively, the following differential equations are obtained [8]:

$$\frac{d^2R}{dt^2} = \frac{p_f}{\rho_f R} \left[ \left( \frac{T_g}{T_f} \right)^{\frac{n}{n-1}} - 1 \right] - \frac{2\sigma_s}{\rho_f R^2} - \frac{3}{2R} \left( \frac{dR}{dt} \right)^2 \quad (10)$$

$$\frac{dT_g}{dt} = - \frac{(n-1)C}{n} \frac{1}{R} \left( \frac{T_f}{\rho_f c_{pg}} \right)^{\frac{1}{n-1}} \left\{ h(T_g - T_f) + \epsilon \sigma_f (T_g^4 - T_f^4) \right\} + T_g \frac{dR}{dt} \quad (11)$$

The initial conditions at  $t=0$  are as follows.

$$R = R_0 \quad \text{and} \quad T_g = T_{g0} \quad (12)$$

$$\frac{dR}{dt} = \sqrt{\frac{2}{3\rho_f} \left( p_{g0} - p_f - \frac{2\sigma_s}{R_0} \right)} \quad (13)$$

$p_{g0}$ ,  $T_{g0}$ , and  $R_0$  appearing in Equation (12) and Equation (13) are the peak over pressure, temperature, and radius of the gas sphere initially, i.e., at time zero. The values of all these three must be prescribed, as they together form the initial condition to solve the differential Equation (10) and Equation (11).

Equations (10) and (11) are solved numerically to obtain the radial distance  $R$  and the gas temperature  $T_g$  as functions of time  $t$  using the initial conditions given by Equations (12) and (13). The gas pressure,  $p_g$  and the density  $\rho_g$  in the blast zone change during the expansion of the blast wave. Hence,  $p_g$  and  $\rho_g$  at each time step are computed

from Equations (8) and (9), respectively. Thus, numerical results are obtained for pressures as functions of time and distance for different weights of TNT and Composition B.

## 2.4 Evaluation of Initial Conditions

The values of  $p_{g0}$ ,  $T_{g0}$  and  $R_0$  (initial radius of blast wave) are computed from blast wave theory [8]. For the blast of 1 kg of TNT,  $p_{g0} = 136.4$  MPa and  $T_{g0} = 2078$  °C. The value of  $R_0 = 0.12$  m when  $p_{g0} = 136.4$  MPa. The initial radius for 1 kg of any other explosive, such as Composition B remains the same. However, the value of  $p_{g0}$  for this explosive will be different since its heat of detonation is different. The initial radii of the blast zone for different weights of the same explosive are calculated making use of the cube root scaling law [9].

## 3 Experimental Section

Experimental firings were conducted in air with explosive charges of different weights to measure the pressure time history of the blast. TNT and Composition B (RDX/TNT/wax 59.5/39.5/1) explosive charges were fired using RDX/wax (95/5) based pressed explosive boosters and electric detonators. Firings were conducted from a remote bunker using low noise cables. The test explosive charge was placed on a wooden stand and held at a height of 2 m from ground for each firing up to 15 kg charge weight. 40 kg cased charges were detonated at a height of 4.5 m. While positioning the blast sensors with respect to scaled distance ( $Z = R/W^{1/3}$ ) care was taken to avoid spurious signals, survivability, and improve the reliability of data [10,11].

Sophisticated instrumentation and measurement techniques were used in the experiments. Omni directional blast pressure pencil probe gauges of PCB, USA make were deployed at different distances from the point of detonation for the measurement of blast pressure. Blast gauges of three different ranges were deployed for the measurements. Gauges (Model 137A21) with a measuring range of up to 7.0 MPa (1000 PSI) were deployed for closer ranges and gauges (Model 137A23) having measuring range up to 0.35 MPa (50 PSI) were deployed for longer distances. Gauges (Model 137A22) of 3.5 MPa (500 PSI) measuring range were deployed for intermediate distances as per requirement, for different weights of explosives. A 16 channel YOKOGAWA make DL 750 high speed data logger was used for acquiring the peak pressure-time data.

## 4 Results and Discussion

Experimental data and numerical results for pressures with distance obtained for different weights of TNT are compared with one another. The theoretical pressures are also obtained for different weights of PBX and Hexotol, which

are compared with the values computed from an empirical equation [12,13], Equation (14), which is modified to suit SI units.

$$P = \frac{0.0662}{Z} + \frac{0.405}{Z^2} + \frac{0.3288}{Z^3} \quad \text{for } 1.0 \leq Z \leq 10.0 \quad (14)$$

for  $1.0 \leq Z \leq 10.0$ , where  $Z = R/W^{1/3}$ .

In addition, temperature is also obtained from the theoretical equations. All these results are presented in figures as follows.

#### 4.1 Results for TNT

The experimental data for the blast in air of 1 kg of TNT are plotted in Figure 2. Theoretical pressures are obtained on computer making use of the analysis for the case of spherical front, viz., for  $C=3$ , by taking  $p_{g0}=136.4$  MPa,  $T_{g0}=2078$  °C and  $R_0=0.12$  m. These results are shown in Figure 2 as broken line. The theoretical results are also obtained using different values of  $C$  between 1 and 3, and it is observed that the results (shown by continuous line) for a value of  $C=2.65$  (a non-spherical curved front) are in well agreement with the experimental data. The reason for the experimental values matching well with theory for a value of  $C=2.65$  may be due to the fact that in actual scenario, the shape of explosive charge used was cylindrical and was end initiated. Thus, the shape of the blast wave was neither perfectly spherical nor plane, but somewhere in between. The model was validated assigning various values for " $C$ " to match the numerical data with experimentally obtained data. This value of 2.65 for " $C$ " was maintained constant for all types of explosive and for all weights from 0.045 kg to 250 kg.

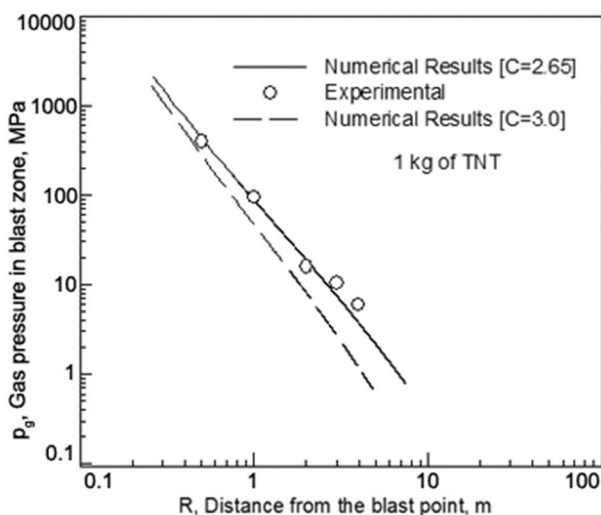


**Figure 2.** Comparison of numerical results of gas pressure in blast zone from theoretical analysis for  $C=3.0$  and  $C=2.65$  with experimental data for 1 kg TNT.

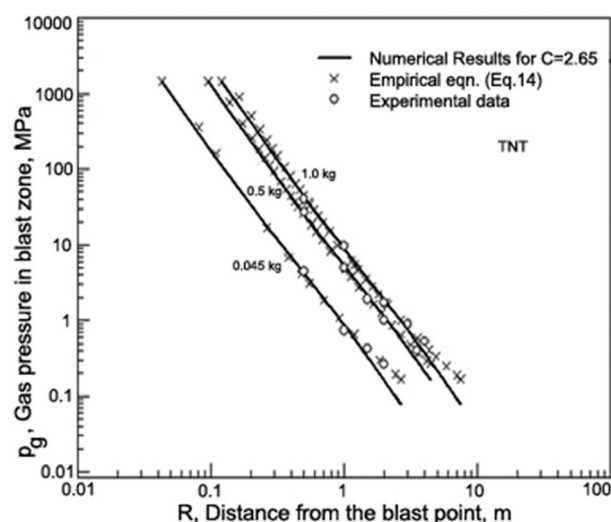


**Figure 3.** Comparison of numerical results of gas pressure in blast zone for  $C=2.65$  with experimental data and empirical equation for 0.045, 0.5, and 1.0 kg TNT.

The numerically obtained pressure data for 0.045, 0.5, and 1.0 kg TNT charges are shown in Figure 3 and are compared with experimental data. The pressures calculated by using Equation (14) for 0.045, 0.5, and 1 kg of TNT are also given in Figure 3. The values of the initial distance  $R_0$  are calculated for the blasts of 0.045 and 0.5 kg TNT making use of the scaled distance  $Z$ . Thus, the values of  $R_0$  obtained are 0.042 and 0.095 m for blast of 0.045 and 0.5 kg TNT, respectively. Theoretical results for 15 and 40 kg TNT charges are shown in Figure 4 in pressure as a function of distance. Figure 4 also shows the comparison of empirically calculated and experimentally obtained pressure data.

Figure 5 shows the comparison of numerical results with the empirical equation, i.e., Equation (14) for 100 and 250 kg TNT charges. The  $R_0$  values for 15, 40, 100, and 250 kg TNT are 0.295, 0.409, 0.556, and 0.756 m, respectively. It can be observed that the numerical results for TNT obtained from the theoretical analysis agree satisfactorily with experimental data for different weights of TNT ranging from 0.045 to 40 kg and also the empirical equation, which is useful by virtue of its simplicity, continues to give points in close agreement with theory. A comparison of theory is made only with results calculated from empirical equation, Equation (14) for 100 and 250 kg, as experimental data are not available.

#### 4.2 Results for Composition B

The theoretical analysis is also tested for Composition B. The heat of detonation for Composition B is computed using the appropriate TNT equivalent given by Cooper [14] and Jeremic and Bajic [15]. Figure 6 shows theoretical results and experimental data for the variation of pressures with distance for 0.045, 0.5, and 1.0 kg Composition B

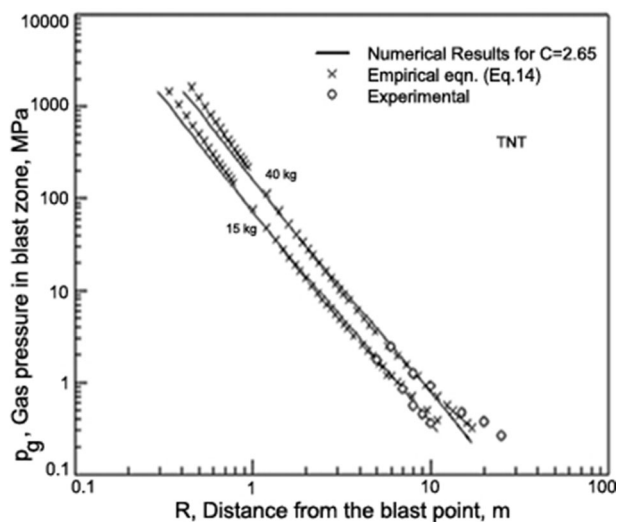


**Figure 4.** Comparison of theoretical results of gas pressure in blast zone for  $C=2.65$  with experimental data and empirical equation for 15 and 40 kg TNT.

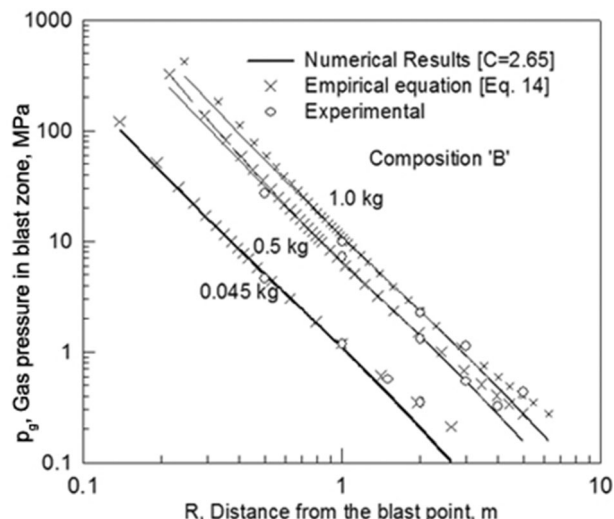


**Figure 6.** Comparison of theoretical results of gas pressure in blast zone for  $C=2.65$  with experimental data and empirical equation, Equation (14), for 0.045, 0.5, and 1 kg of Composition B.

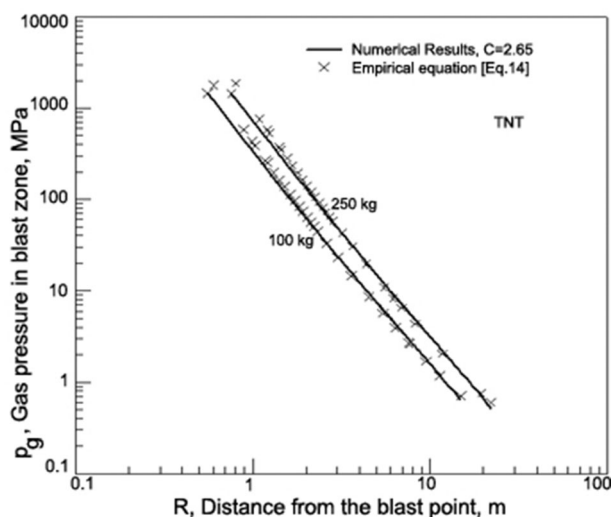


**Figure 5.** Comparison of theoretical results of gas pressure in blast zone for  $C=2.65$  with empirical equation, Equation (14), for 100 and 250 kg TNT.

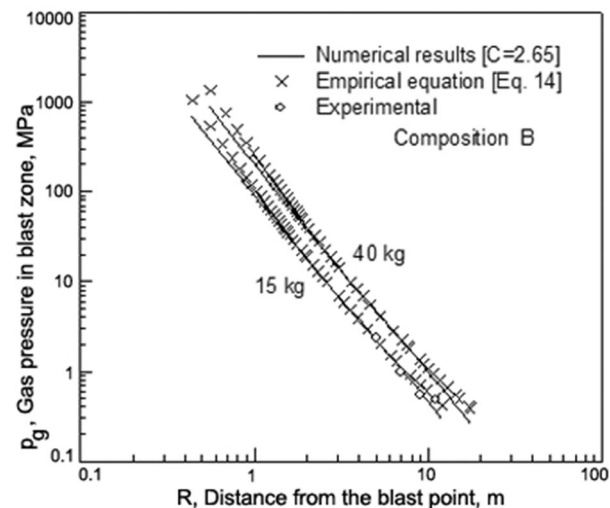


**Figure 7.** Comparison of theoretical gas pressure in blast zone for  $C=2.65$  with experimental data and empirical equation, Equation (14), for 15 and 40 kg of Composition B.

charges. Figure 6 also shows a comparison with the empirically calculated values from Equation (14). The numerical for pressures of blast of 15 and 40 kg Composition B charges results are shown in Figure 7 along with the experimental data for 15 kg charge. Pressures calculated from Equation (14) for 15 and 40 kg of Composition B are also shown in Figure 7. It is observed that the theoretically predicted pressures are in well agreement with the experimental as well as the empirical values.

The comparison was done up to the validity range with respect to  $Z$  of the empirical Equation (14).

A practical application of these results can be explained as follows. A peak over pressure of 1 MPa is required to cause damage to a concrete structure [16–18]. TNT charges of 10 kg and 50 kg weight are required to cause damage to the concrete structures at distances of 2 m and 5 m, respectively. Thus, the results for pressure vs. distance (presented in Figure 3 and Figure 4 for TNT and Figure 7 for Composition B) can be used to predict the damage potential of these explosives. The results of this study can be used to compute the impulses created by different weights of explosives.

## 5 Conclusions

A theoretical model to predict the pressure generated in the blast wave due to detonation of high explosives in air at any distance from the center of explosion is developed. It is validated by the experimental data of TNT and Composition B for various weights of each explosive ranging from 0.045 kg to 40 kg, and an empirical equation available in literature with the aid of TNT equivalents for the explosives. The theory outlined herein helps in predicting the pressures at shorter distances from the blast point.

## Nomenclature and Symbols

RDX	Cyclotrimethylene trinitroamine
TNT	Trinitrotoluene
$Q$	Heat of detonation [ $\text{kJ kg}^{-1}$ ]
$C$	Curvature factor defined in Equation (11), $C=3$ (spherical front), $C=1$ (plane front)
$g$	Gravitational constant [ $\text{m s}^{-2}$ ]
$h$	Convection heat transfer coefficient [ $\text{W m}^{-2} \text{K}^{-1}$ ]
$k$	Thermal conductivity [ $\text{W m}^{-1} \text{K}^{-1}$ ]
$n$	Exponent of polytropic process as defined in Equation (14)
$p$	Pressure [ $\text{N m}^{-2}$ ]
$r$	Position coordinate [m]
$R$	Distance from blast point to gas-to-fluid interface [m]
$Z$	Scaled distance [ $\text{RW}^{-1/3}$ ]
$t$	Time [s]
$T$	Temperature [K]
$U$	Velocity of fluid [ $\text{m s}^{-1}$ ]

## Greek Symbols

$\varepsilon$	Emissivity
$\rho$	Density [ $\text{kg m}^{-3}$ ]
$\rho_g$	Density of gas at temperature $T_f$ [ $\text{kg m}^{-3}$ ]
$\sigma_s$	Surface tension [ $\text{N m}^{-1}$ ]
$\sigma_r$	Stefan-Boltzmann constant ( $5.67 \times 10^{-8} \text{ W m}^{-2} \text{ K}^4$ )

## Subscripts

0	initial
f	fluid
g	gas
i	gas-to-fluid interface

## Acknowledgments

The authors thank Dr. A. Subhananda Rao, Director, High Energy Materials Research Laboratory, Pune for providing explosives and experimental facilities. The authors thank all the Scientists/Officers

of HEMRL, Pune who helped in conduct of the experiments. The authors also thank Mr. A. Jagannadham, NSTL, Visakhapatnam who helped in preparation of this paper.

## References

- [1] C. E. Needham, *Blast Waves, Shock Wave and High Pressure Phenomena*, Springer-Verlag Berlin Heidelberg, **2010**, pp. 42.
- [2] A. H. Shapiro, *Compressible Fluid Flow*, Vols. 1, 2, John Wiley & Sons, Hoboken, **1953**.
- [3] P. H. Oosthuizen, E. William Carscallen, *Compressible Fluid Flow*, McGraw-Hill New York, **1997**.
- [4] V. Krishna Mohan, T. B. Tang, Explosive Performance Potential – A New Definition, *Propellants Explos. Pyrotech.* **1984**, 9, 30–36.
- [5] S. Watson, W. N. Macpherson, J. S. Barton, J. D. C. Jones, A. Tyas, A. V. Pichugin, A. Hindle, W. Parkes, C. Dunare, T. Stevenson, Investigation of Shock Waves in Explosive Blasts using Fibre Optic Pressure Sensors, *Meas. Sci. Technol.* **2006**, 17, 1337–1342.
- [6] L. Yu, K. Deren, Storage Measurement System for Explosion Temperature, *Int. Conference on Measuring Technology and Mechatronics Automation*, Wuhan, China, March 13–14, **2010**, pp. 496–498.
- [7] R. H. Cole, *Underwater Explosions*, Dover Publications, New York, **1965**, 122.
- [8] A. Srinivas Kumar, V. Dharma Rao, K. Venkateswara Rao, V. S. R. Krishna Prasad, V. Bhujanga Rao, Theoretical Prediction of Pressure and Temperature of an Aluminized High Explosive in Underwater Explosion, *Propellants Explos. Pyrotech.* **2014**, 39, 224–229.
- [9] W. E. Baker, *Explosions in Air*, University of Texas Press, Austin, **1973**.
- [10] E. D. Esparza, Blast Measurements and Equivalency for Spherical Charges at Small Scaled Distances, *Int. J. Impact Eng.* **1986**, 4, 23–40.
- [11] K. Cheval, O. Loiseau, V. Vala, Laboratory Scale Tests for the Assessment of Solid Explosive Blast Effects, Part I: Free-Field Test Campaign, *J. Loss Prevention Process Ind.* **2010**, 23, 613–621.
- [12] J. Henrych, *Dynamics of Explosion*, Elsevier, Amsterdam, **1979**.
- [13] K. Harbanslal, S. K. Vasudeva, Directional Effects of Explosions in One Sided Open Cubicle Structures, *IMPLAST 2010 Conference*, October 12–14, **2010**, Providence, RI, USA.
- [14] P. W. Cooper, Comments on TNT Equivalence, *20th International Pyrotechnics Seminar*, July 25–29, **1994**, Colorado Springs, CO, USA, pp. 1–12.
- [15] R. Jeremic, Z. Bajic, An Approach to Determining the TNT Equivalent of High Explosives, *Scientific Technical Review*, **2006**, VI (1), pp. 58–62.
- [16] D. Jiang, Y. Liu, Z.-D. Ma, B. Raju, Development of a Blast and Fragment Model for Simulating Land Explosives, *ASME 2007, International Mechanical Engineering Congress and Exposition (IMECE2007)*, Mechanics of Solids and Structures, Parts A and B, Seattle, WA, USA, October 11–15, **2007**, pp. 585–592.
- [17] M. Held, Blast Waves in Free Air, *Propellants Explos. Pyrotech.* **1983**, 8, 1–7.
- [18] M. Held, TNT-Equivalent, *Propellants Explos. Pyrotech.* **1983**, 8, 158–167.

Received: February 15, 2014

Revised: July 31, 2014

Published online: September 10, 2014